Published in final edited form as:
Neurobiol Dis. 2014 April ; 64: 107–117. doi:10.1016/j.nbd.2014.01.007.

Synergistic effects of amyloid-beta and wild-type human tau on dendritic spine loss in a floxed double transgenic model of Alzheimer's disease

Meredith A. Chabrier[1], **David Cheng**, **Nicholas A. Castello**[1], **Kim N. Green**, and **Frank M. LaFerla**

Institute for Memory Impairments and Neurological Disorders, and Department of Neurobiology and Behavior, University of California, Irvine, Irvine, California, 92697-4550

Abstract

Synapse number is the best indicator of cognitive impairment In Alzheimer's disease (AD), yet the respective contributions of Aβ and tau, particularly human wild-type tau, to synapse loss remain undefined. Here, we sought to elucidate the Aβ-dependent changes in wild-type human tau that trigger synapse loss and cognitive decline in AD by generating two novel transgenic mouse models. The first overexpresses floxed human APP with Swedish and London mutations under the thy1 promoter, and recapitulates important features of early AD, including accumulation of soluble Aβ and oligomers, but no plaque formation. Transgene excision via Crerecombinase reverses cognitive decline, even at 18-months of age. Secondly, we generated a human wild-type tau-overexpressing mouse. Crossing of the two animals accelerates cognitive impairment, causes enhanced accumulation and aggregation of tau, and results in reduction of dendritic spines compared to single transgenic hTau or hAPP mice. These results suggest that Aβ-dependent acceleration of wild-type human tau pathology is a critical component of the lasting changes to dendritic spines and cognitive impairment found in AD.

Keywords

Alzheimer's disease; wild-type tau; dendritic spines; transgenic

INTRODUCTION

Amyloid-beta (Aβ) and tau, the primary proteins implicated in Alzheimer's disease (AD) pathology, accumulate and form insoluble plaques and tangles, respectively (Querfurth and

Corresponding author: Frank M. LaFerla, laferla@uci.edu, 3212 Biological Sciences III, University of California, Irvine, Neurobiology and Behavior, Irvine, CA 92697-4550. Phone: (949) 824-1232.
[1]Present address: Gladstone Institute of Neurological Disease, University of San Francisco, San Francisco, California, 94158

Conflicts of interest: The authors declare no competing financial interests.

LaFerla, 2010). The relationship between the toxic, soluble intermediates of these proteins and their impact on cognition, however, is poorly understood. Loss of excitatory synapses, as opposed to the plaque and tangle load, correlates with cognitive impairment in AD patients (DeKosky and Scheff, 1990; Terry et al., 1991). Interestingly, the areas of synaptic loss are the same areas where neurodegeneration occurs, suggesting that neuronal loss is a secondary consequence of the same factors that trigger loss of synapses. Discerning the biological causes of early synaptic dysfunction in AD is a significant question in the field, as the downstream effects of protein accumulation, synapse loss and neurodegeneration have proved too extensive to properly treat with single therapeutics (Pillai and Cummings, 2013).

Soluble Aβ oligomers are potent mediators of synaptotoxicity, and localize rapidly to the synapse in cultured neurons and mouse models of AD (Deshpande et al., 2006; Zempel et al., 2010). Depending on the concentration and aggregation state, Aβ can either enhance presynaptic activity or depress post-synaptic activity through activation of multiple receptor pathways (Mucke and Selkoe, 2012). Recent studies indicate that tau is a critical mediator of Aβ-induced synaptotoxicity, as removing endogenous tau from human APP mouse models prevents the cognitive deficits and synaptic loss found when murine tau is present (Roberson et al., 2007). One proposed pathway by which tau may mediate synaptotoxicity is through interactions with the protein kinase Fyn. Tau binds Fyn, transporting it to the post-synaptic density where it phosphorylates the NR2B subunit of NMDARs, stabilizing the interaction between NMDARs and PSD-95. (Lee et al., 1998; Salter and Kalia, 2004; Ittner et al., 2010). This stabilization could enhance Aβ induced toxicity through NMDARs. Importantly, knockdown of Fyn in Aβ-treated slice cultures and APP transgenic mice mitigates synaptic deficits (Lambert et al., 1998; Chin et al., 2004).

Several studies have shown that Aβ promotes tau hyperphosphorylation and aggregation (Gotz et al., 2001, Lewis et al., 2001). The triple transgenic 3xTg-AD model created in our laboratory greatly advanced the field in this area by providing an *in vivo* model with both Aβ and tau pathology, synaptic dysfunction, and cognitive decline with age. Using this model, we determined that Aβ pathology precedes tau pathology (Oddo et al., 2003a), and that immunotherapy targeting Aβ can ameliorate both Aβ and soluble tau pathology (Oddo et al., 2004). However, all of these models utilize mutant forms of tau, begging the question whether the wild-type human form of tau found in AD is susceptible to the same Aβ driven mechanisms.

Here, we sought to elucidate the Aβ-dependent changes in wild-type human tau that cause synaptic loss and cognitive decline in AD, focusing on changes in synaptic proteins in the Fyn kinase pathway. We generated novel single transgenic mouse models expressing human wild-type tau and floxed human APP, and crossed these models to compare changes in tau and synapse pathology between the double and single transgenic models. Interestingly, reducing APP in the single transgenic human APP model rescues cognition at advanced stages in the disease course, but the presence or absence of APP does not alter levels of synaptic markers in this model. In contrast, we find that crossing human APP mice to human wild-type tau mice accelerates cognitive impairment, causes enhanced accumulation and aggregation of tau, and results in reduction of dendritic spines compared to single transgenic

hTau or hAPP mice. These data suggest that accumulation of wild-type human tau is a critical component of Aβ-dependent synaptotoxicity.

MATERIALS AND METHODS

Generation of transgenic mice

APP695 cDNA with Swedish and London mutations, as well as flanking loxP sites, was synthesized by Bio Basic, Inc. (Markam, Ontario, Canada). Full-length human tau 2N/4R cDNA was used previously in our models (Chabrier et al., 2012) and was originally a gift from Dr. Michael Vitek. $hAPP_{SL}$ and hTau constructs were subcloned into the Thy1.2 expression cassette (Caroni, 1997) using a homologous recombination approach (Clonetech, In-Fusion). Sequence-verified clones were digested to liberate the targeting cassette and purified by gel extraction. Thy1-$hAPP_{SL}$ and Thy1-hTau constructs were then respectively injected into the pronuclei of single-cell C57Bl6 embryos by the UC Irvine Transgenic Mouse Facility, creating two single transgenic models with multiple founder lines.

Breeding and genetic analysis of founder lines

All animal procedures were performed in strict accordance with NIH and University guidelines. Mice were housed on a 12 hr light/dark schedule with ad libitum food and water. Transgenic mice were identified by tail PCR, and nontransgenic littermate controls were generated by crossing hemizygous transgenics with wild-type C57/Bl6 mice (Taconic Farms, Inc). The percentage of nontransgenic versus transgenic mice was tracked for each generation of offspring to ensure normal integration and inheritance of the transgene. Southern blots were additionally performed on genetic DNA from each founder to ensure proper integration of the transgene. $hAPP_{SL}$ founder DNA was digested with EcoRI, with an excepted transgene band at 6 kb. hTau founder DNA was digested with HindIII, with expected bands at 6, 6.4, and 6.8 kb.

Cognitive and behavioral tasks

Several different tasks were performed to assess anxiety, learning and memory, and motor skills in nontransgenic, single transgenic, and double transgenic mice. The mice were age and sex-matched for all testing.

Open field testing was performed by placing a mouse in an open plastic container with 4 white walls and no bedding on the floor. A camera was situated directly above the container to film the mouse during its 5 minutes in the box. The box was cleaned with 70% ethanol between each mouse. This was repeated for three days, and then the videos were run through Noldus XT for analysis of the total distance moved each day.

Novel object recognition was performed following further habituation after open field. Two identical objects (clear 100mL beaker or yellow small dumbbell) were equally spaced in the same white boxes. On training day, the mouse was placed into the box and allowed to explore both objects for 5 minutes. On testing day, one of the objects (either the beaker or dumbbell) was replaced with a novel object and the mouse was placed back in the box and allowed to explore for 3 minutes. Both days were filmed, and the total time spent with each

object was analyzed on both training and test days. The discrimination index, or preference for the novel object, was determined by calculating: ($Time_{novel} - Time_{old}$)/($Time_{novel} + Time_{old}$), where 0 equals no preference for either object.

Mice were then tested on Rotarod for motor impairments. Animals were placed on a Rotarod apparatus for 5 trials, with 10 minutes between trials. The rod accelerated from 4 to 40 rpm over 5 minutes, and the time at which the mouse fell off the rod was recorded, with a 5 minute maximum. The rod was cleaned with 70% ethanol between trials.

Finally, hippocampus dependent learning and memory was assessed by either Barnes maze or Morris water maze. For Barnes maze, a hidden escape box was placed below one of 40 circular holes evenly spaced around a raised circular platform, 120 cm in diameter. Four large distinct cues were placed on each wall surrounding the platform. For the first trial, the mouse was placed under a box on the center of the platform for 15s, after which the box was removed and the mouse was allowed to explore the platform for 2 minutes. If the mouse did not find the escape box, it was led to the box. Once in the box, the hole was immediately covered, the box was removed, and the mouse was placed back in its home cage. Animals were given 2 trials per day over four days, with a 10-minute intertrial interval.

For Morris water maze, male and female 8-month old animals were habituated to a 1.5-meter diameter circular pool filled with opaque water maintained at 29°C. During training, mice were placed into the pool and allowed to find a submerged escape platform for 4 trials per day. Four large distinct cues were placed on each wall surrounding the pool. After four days of training, the platform was removed and mice were tested 24 hours later to assess memory retention for the former platform location.

Tissue Processing

Mice were sacrificed by Euthasol overdose and cardiac perfusion with 0.01 M phosphate buffered saline (PBS). Brains were removed and cut along the sagittal midline. Half the brain was microdissected into hippocampus, cortex, and cerebellum and were frozen on dry ice for subsequent biochemical analysis, while the other half was fixed in 4% paraformaldehyde (pH-7.4, 48 hrs). Fixed half-brains were cut in 40 μm thick coronal sections on a microtome and stored in PBS with 0.02% NaN_3 at 4°C until use.

Biochemical analysis

Microdissected samples were processed to isolate soluble (T-PER) and insoluble (70% formic acid) protein from each animal following standard protocols (Oddo et al., 2007). Soluble and insoluble SDS-page western blots and Aβ sandwich ELISAs were also performed as previously described (Blurton-Jones et al., 2009). The following primary antibodies were used: 6E10 (Covance, Princeton, NJ), GAPDH (Santa Cruz Biotech, Dallas, TX), HT7 (Pierce, Rockford, IL), AT180 (Pierce, Rockford, IL), Tau46 (Cell Signaling, Danvers, MA), synaptophysin (Sigma, St. Louis, MO), PSD-95 (Abcam, Cambridge, MA), Fyn (Abcam, Cambridge, MA), pFyn530 (Abcam, Cambridge, MA), CT20 (Millipore, Billerica, MA), GSK3β (BD Biosciences, San Jose, CA), pGSK3βSer9/Ser21 (Cell Signaling, Danvers, MA), CDK5 (Millipore, Billerica, MA), JNK (Cell Signaling, Danvers, MA), pJNK (Cell Signaling, Danvers, MA), p35/25 (Santa Cruz Biotech, Santa Cruz, CA)

NR2B (Millipore, Billerica, MA), pNR2BY1472 (Sigma, St. Louis, MO). Dot blots to recognize amyloid oligomers were performed with 2 μg of protein per sample using conformational-dependent antibody OC (gift of C. Glabe).

Immunofluorescence and Confocal Microscopy

Free-floating sections were washed in TBS, and then incubated TBS + 0.1% Triton X-100, followed by block (TBS with 0.2% Triton X-100, 3% BSA, and 3% normal goat serum) for 1 hr. Sections were incubated overnight at 4°C in primary antibodies diluted in TBS with 3% BSA and 3% goat serum. On day 2, sections were washed 3 times in TBS followed by 1 hr incubation at room temperature in Alexa Fluor fluorescent secondary antibodies (1:200, Life Technologies, Grand Island, NY). The following primary antibodies were used: MAP2 (Millipore, Billerica, MA), Aβ42 (Biosource, Life Sciences) NeuN (Millipore, Billerica, MA), 6E10 (Covance, Princeton, NJ), CT20 (Millipore, Billerica, MA), synaptophysin (Sigma, St. Louis, MO), PSD-95 (Abcam, Cambridge, MA), HT7 (Pierce, Rockford, IL) polyclonal tau (DAKO, Carpinteria, CA), PHF-1 (Gift of Peter Davies). Finally, sections were mounted onto slides and coverslipped in Flouromount (Southern Biotech, Birmingham, AL). Immunofluorescently labeled sections were imaged with a Leica DM2500 TCS SPE laser scanning confocal microscope. Identical scan settings were used for all samples for each brain region analyzed. Images were analyzed using ImageJ software (NIH).

Bitplane Imaris software analysis

Analysis of PSD-95 and synaptophysin confocal images was performed using the spot module of Bitplane Imaris software ver. 7.5.2. The estimated diameter was set at 0.3 μm.

Golgi staining and spine quantification

Golgi staining was performed using SuperGolgi Kit (Bienno Tech, Santa Ana, CA). Briefly, brains were incubated in impregnation solution for 11 days following perfusion. Coronal sections of 100 μm were cut on a Vibratome and collected on gelatin-coated microscope slides. The sections were stained and then coverslipped with DPX (Sigma, St. Louis, MO). High-precision design based stereology was used to quantify and classify the number of dendritic spines in the stratum radiatum. Spine numbers and types were determined on a stereology workstation (StereoInvestigator, MicroBrightField, Williston, VT, USA). The investigator was blinded for the treatment and genotype of the animals, and all counts were done by the same investigator. On every 2nd section, the area of interest was delineated using the 5X objective, and was divided into counting frames of 25 μm by 25 μm using the Optical Fractionator probe. The scan grid size was 150 μm by 150 μm, so that each region of interest contained approximately 18–22 scanning sites. Four sections per animal were counted. Spines were counted using the 100X oil-immersion objective, and classified as either mushroom, stubby, or thin based on previously established criteria (Chen et al, 2010). The guard zone was set at 5 μm and total distance counted through the section at 35 μm. This counting scheme resulted in counting approximately 2000 spines per animal, and Gunderson coeffecient of error values less than 0.09 for each spine classification.

Statistical Analysis

Comparisons between multiple groups were performed using analysis of variance (ANOVA) followed by Bonferroni post-hoc tests. Error bars represent +/− SEM. Analysis of Barnes maze and MWM acquisition were examined via repeated-measured ANOVA. Groups were considered significantly different when *$p<0.05$ for both the ANOVA and posthoc comparisons. Comparisons between two groups utilized unpaired Student's *t* test. All statistical analysis was performed using GraphPad Prism software (San Diego CA).

RESULTS

Generation of $hAPP_{SL}$ mouse model exhibiting increasing Aβ accumulation and cognitive deficits with age

We generated a novel model of early-stage AD by cloning human APP-695 with Swedish and London mutations into the Thy1.2 promoter cassette to create a construct that produces moderate levels of Aβ specifically in neurons in AD relevant brain regions. (Figure 1A). To study the effects of APP removal at different time points during the disease course, we added loxP sites flanking the APP transgene, allowing for excision of the transgene upon exposure to Cre recombinase. Breeding and Southern blot analyses suggested that of the five possible founders, lines A1 and A3 had proper integration of the transgene (data not shown). Further analyses showed that line A3 had robust expression of APP and APP cleavage products (Figure 1B), and this was the chosen as the candidate founder line for future experiments. $hAPP_{SL}$ hemizygous mice from line A3 exhibit almost 4-fold overexpression of APP over endogenous levels, and similar levels of cortical overexpression to homozygous 3xTg-AD mice, whereas 3xTg-AD mice have increased levels in the hippocampus (Figure 1B–C). Importantly, OC-positive prefibrillar oligomers are evident in $hAPP_{SL}$ mice, and accumulate with age (Figure 1D). $hAPP_{SL}$ mice never exhibit congophilic or ThioS positive plaques, but they do accumulate increasing levels of APP, soluble Aβ and insoluble Aβ (Figure 1E–G). This finding is consistent with other inbred APP models with low levels of APP expression and without the presenilin mutation (Carlson et al., 1997). Interestingly, despite the cognitive deficits observed at 12 months in this model, there are no differences in synaptic markers PSD-95 and synaptophysin with age (Figure 1H–I). Because the triad of Aβ, tau, and the protein kinase Fyn has been implicated in synaptoxocity, we also examined levels of Fyn and its substrate NR2B (Ittner et al 2010, Chabrier et al. 2012). Levels of the NMDAR subunits NR2B are significantly elevated at 12 months of age compared to young 3 month $hAPP_{SL}$ mice, while a trend toward increased phosphorylated NR2B at tyrosine-1472 is observed at 18 months of age (Figure 1I).

Cre AAV ablates APP expression and rescues cognition

To examine whether removing APP from aged $hAPP_{SL}$ mice could rescue cognitive deficits, we utilized the loxP sites and excised the APP transgene in 18-month old $hAPP_{SL}$ mice by injecting adeno-associated virus (AAV) expressing Cre recombinase (Figure 2A). By immunofluorescent staining for human APP, we found a 95% reduction of APP expression in the CA1 pyramidal cell layer, while no changes were observed in cortical areas (Figure 2B–F). Western blot analysis of microdissected hippocampi samples showed a 50% reduction of APP throughout the entire hippocampus (Figure 2G). Four to five weeks post

hippocampal-injections, $hAPP_{SL}$ mice with Cre ($hAPP_{SL}$/Cre) performed significantly better in cognitive tasks than $hAPP_{SL}$ mice injected with vehicle (hAPP, Figure 2H–I). As shown by Barnes Maze, reduced APP expression in hAPP/Cre mice led to successful learning and memory that was equivalent to the performance of nontransgenic mice. In contrast, hAPP mice injected with vehicle performed significantly worse than nontransgenics in both the learning and 24-hour memory tasks (Figure 2H–I). These data indicate that in a model of human APP accumulation, with no human tau pathology present, removing APP even at advanced stages of disease progression is sufficient to ameliorate cognitive deficits.

Dendritic mislocalization of tau leads to synapse loss and cognitive decline in wild-type human tau transgenic mice

To investigate the different effects of APP and tau on cognition and synaptic pathology, we created a wild-type human tau mouse to cross to the $hAPP_{SL}$ model (Figure 3A). This mouse harbors the same transgene as a previous model (Gotz et al., 1995), but exhibits slightly different pathological and behavioral phenotypes, as is the case with every new transgenic founder line. Similar to the $hAPP_{SL}$ line, we completed breeding and southern blot analysis before deciding on a candidate founder line (data not shown). After deciding on the T1 founder line, we analyzed total tau and tau phosphorylation levels in hemizygous hTau animals compared to homozygous 3xTg-AD, which harbors a presenilin 1 mutation, human APP transgene, and the 4R/0N form of human tau with the P301L mutation. hTau mice exhibited similar total tau expression, but less tau phosphorylation than 3xTg-AD mice, as expected in a mouse with no mutations in tau and no Aβ present (Figure 3B). hTau mice exhibit somatic mislocalization of tau at 6 months, most prominently in the amygdala and cortex, but also in hippocampal regions CA1 and CA3 (data not shown). Hyperphosphorylated tau at pSer396/404 (PHF-1 positive) also increased with age, moving to the somatodendritic compartments in almost all wild-type human tau positive cells in CA1 at 18 months (Figure 3C–D). Cognitive deficits are not evident in hTau mice until 18 months of age, as seen by deficits in novel object recognition (Figure 3E). Biochemical studies reveal that steady-state levels of soluble tau remain constant with age, but there is a significant decrease in the post-synaptic marker PSD-95 at 18 months, consistent with the timepoint of cognitive decline (Figure 3F–G). Interestingly, we also see a significant increase in phosphorylated NR2B at 18 months, which has been suggested to contribute to synaptotoxicity in AD models (Ittner et al., 2010). To investigate the aggregation state of tau with age, we performed western blots with the insoluble fractions and probed for total tau and phosphorylated tau. Total insoluble tau deposits were found to be increased at 18 months, while no differences were seen in levels of insoluble phosphorylated tau at PHF-1 epitope pSer396/404 (Figure 3H–I).

Acceleration of cognitive deficits in double transgenic $hAPP_{SL}$/hTau mice

$hAPP_{SL}$ mice were bred with hTau mice, resulting in offspring of the following genotypes: nontransgenic, hemizygous $hAPP_{SL}$, hemizygous hTau, and hemizygous $hAPP_{SL}$/Tau. Age and sex-matched mice from each genotype were aged to 8 months, an age where cognitive deficits were not yet evident in single transgenic mice, and then analyzed for cognitive and pathological differences.

Animals were first analyzed for anxiety and the ability to habituate to a context through three days of open field tests. By day 3, nontransgenic and hTau mice showed less exploratory movement, while $hAPP_{SL}$ and $hAPP_{SL}$/hTau mice moved significantly more, indicating higher anxiety and less habituation to the context (data not shown). To ensure that any differences in behavior were not due to motor deficits, the mice were tested on a Rotarod for five consecutive trials. Importantly, no differences were observed between groups, suggesting that none of the groups exhibited any motor deficits (Figure 4A). Mice were then evaluated for hippocampus-independent learning and memory by using novel object recognition task. All groups spent an equivalent amount of time exploring the objects on training and testing days; however, nTg, hTau, and $hAPP_{SL}$ mice all displayed a significant preference for the novel object on test day, while $hAPP_{SL}$/hTau mice showed no preference, suggesting no memory for the previous objects (Figure 4B). To further test for differences in cognition, mice were tested in the hippocampus-dependent task Morris water maze. Again, the swim speeds between groups were all equivalent, indicating motor competency in all mice (Figure 4C). After four days of 4 trials per day, all groups reached the criterion of finding the platform in less than 25 seconds except $hAPP_{SL}$/hTau mice, who took significantly longer than nTg mice (Figure 4D). On the fifth day, the platform was removed and the mice were tested for their memory of the platform location. Consistent with the acquisition data, $hAPP_{SL}$/hTau mice crossed the platform location significantly less than nTg mice (Figure 4E). There were no significant differences between either $hAPP_{SL}$ or hTau groups and nTg mice. $hAPP_{SL}$/hTau mice also trended towards at increased latency for the platform during the probe trial test, on average taking 10 seconds longer than nTg mice to find the platform location (Figure 4F).

The presence of human APP increases tau accumulation in $hAPP_{SL}$/hTau mice

To examine the effects of APP and its derivatives on wild-type tau pathology, we compared levels of APP and human tau accumulation in the hippocampus between all four groups. Levels of human tau were significantly increased in $hAPP_{SL}$/hTau mice compared to single transgenic hTau mice, while total levels of APP were unchanged between $hAPP_{SL}$/hTau and single transgenic $hAPP_{SL}$ mice (Figure 5A–E). Interestingly, no differences were observed in soluble phosphorylated tau (data not shown), or in the major tau kinases GSK3β, CDK5, JNK or phosphatase PP2A (Figure 5F). However, both total tau and tau phosphorylated at pSer396/404 were increased in the insoluble fraction of hAPP/hTau mice compared to hTau mice, indicating that the presence of human APP and Aβ enhances tau accumulation and aggregation in human wild-type tau mice (Figure 5G – H).

Reduction of dendritic spines in $hAPP_{SL}$/hTau mice

We next investigated the differences in synaptic pathology between groups by Golgi staining. Using unbiased stereology, we assessed spine density in the stratum radiatum layer of the hippocampus in each group. We found a 35% decrease in spine density in $hAPP_{SL}$/hTau mice compared to nTg, significantly less than all other groups (Figure 6A–B). Spines were classified into three generalized subtypes: mushroom (neck and head), thin (neck with no head), and stubby (head with no neck). Interestingly, the decrease in spine density in $hAPP_{SL}$/hTau mice was almost exclusively due to a lack of mushroom type spines (Figure 6C).

The marked change in dendritic spine density led us to examine differences in synaptic proteins that have previously been implicated in Aβ and tau pathology. Importantly, a decrease in the number of synapses in $hAPP_{SL}$/hTau mice was found by labeling with PSD-95 and counting the number of puncta in the stratum radiatum (Figure 6D–F). This finding was further confirmed by western blot of hippocampal samples from each group (Figure 6I–J). No differences in the pre-synaptic markers synaptophysin were observed using the same techniques. Interestingly, we found a significant increase in the protein kinase Fyn in $hAPP_{SL}$/hTau mice, which has been shown to phosphorylate NR2B receptors, possibly leading to enhanced Aβ-mediated excitotoxicity. Despite the profound loss of dendritic spines, we observed a trending increase in NR2B, as well as phosphorylated NR2B at tyrosine-1472, in $hAPP_{SL}$/hTau mice. Additionally, no differences were found in the levels of neuronal marker NeuN between $hAPP_{SL}$/hTau and nTg mice, indicating that the loss of spines is not due to overt neuronal loss (Figure 6K–M).

DISCUSSION

Synapse loss is the best pathological correlate of cognitive decline in AD, but the roles of the hallmark protein pathologies, Aβ and tau, in facilitating synapse loss remain unclear (Koffie et al., 2011). Mounting evidence demonstrates localization of Aβ with synaptic markers, where Aβ may have a role in regulating normal synaptic transmission (Kamenetz et al., 2003), but upon aberrant accumulation of Aβ oligomers, this synaptic interaction becomes toxic. Transgenic mouse models of hAPP have shown synaptotoxicity due to accumulation of soluble oligomeric Aβ, before evidence of plaque accumulation (Mucke et al., 2000; Lesne et al., 2006), as well as increased synapse loss near dense core plaques (Spires et al., 2005). It is likely that different forms of Aβ have varying roles in targeting synaptic receptors, making this a difficult therapeutic target depending on the stage of disease progression (Larson and Lesne, 2012).

To understand the efficacy of targeting Aβ at various stages of AD pathology, we generated a new transgenic mouse model with a floxed human APP transgene that produces increasing levels of soluble and insoluble Aβ as well as Aβ oligomers with age. Introducing Cre recombinase into the neurons of these $hAPP_{SL}$ mice allows for excision of the transgene. Interestingly, these mice develop cognitive deficits without any observable changes in synaptic density, possibly indicating that Aβ is impairing synaptic function by exacerbating synaptic channels, such as NR2B containing NMDA receptors, without overt changes in the number of synapses. Removing APP and Aβ expression reverses the cognitive deficit in $hAPP_{SL}$ mice. However, the critical question remains as to whether targeting APP and Aβ in the presence of wild-type tau pathology will still rescue cognitive deficits. To begin to investigate this question, we crossed $hAPP_{SL}$ mice with hTau mice and examined these mice for changes in cognition and pathology at 8 months of age, before any cognitive deficits are seen in either single transgenic line. $hAPP_{SL}$/hTau double transgenic mice exhibit learning and memory deficits in two different cognitive tasks, novel object recognition and Morris water maze. Next, we examined the changes in pathology that could be causing this acceleration of cognitive decline. We found a 50% increase in tau accumulation in $hAPP_{SL}$/hTau mice compared to hTau, whereas no changes were found in human APP levels. No changes in levels of soluble phosphorylated tau between groups, or in activity of critical tau

kinases were found; however, an increase in insoluble, hyperphosphorylated tau was found in $hAPP_{SL}$/hTau mice compared to hTau mice alone. Based on our investigations of single transgenic hAPP, single transgenic hTau and the crossed double transgenic hAPP/hTau, we can conclude that human wild-type tau alone becomes hyperphosphorylated with age, but the presence of Aβ facilitates accumulation of both soluble and insoluble tau, and increases tau mislocalization.

Once mislocalized, wild-type human tau may mediate post-synaptic toxicity through modulation of receptor stabilization (Hoover et al., 2010; Ittner et al., 2010; Chabrier et al., 2012; Mairet-Coello et al., 2013). Interestingly, we found an upregulation of Fyn kinase in $hAAPP_{SL}$/hTau mice, but no changes were found in Fyn in either single transgenic line alone. Concomitant with Fyn upregulation, we found a significant decrease in the postsynaptic marker PSD-95 as well as a marked reduction of mushroom spines in the stratum radiatum of $hAPP_{SL}$/hTau mice compared to nontransgenic, $hAPP_{SL}$, and hTau mice. Mushroom spines have been termed “memory spines” as they have larger post-synaptic densities that anchor more excitatory AMPA receptors, allowing them to be functionally strong and stable for long periods (Kasai et al., 2003; Holtmaat et al., 2006). Selective loss of these spines has been correlated with cognitive decline in several models of Aβ or tau pathology, respectively (Dickstein et al., 2010; Perez-Cruz et al., 2011). Importantly, we show that accumulation of both Aβ and wild-type human tau synergistically impairs dendritic spines in the hippocampus. Moreover, the loss of synapses, as seen by a decrease in post-synaptic marker PSD-95, occurs concurrently with dramatic mislocalization of tau and enhanced insoluble tau deposition, whether in aged hTau mice or in the accelerated $hAPP_{SL}$/hTau mice. From a therapeutic standpoint, this indicates that we need to target these proteins before they exert their synaptotoxic effects, which is likely well-before AD is diagnosed (Jack et al., 2010). Once disease pathology progresses to a cascade of Aβ, tau and dendritic spine loss, it is likely too late to reverse these structural changes. Future studies will illuminate whether simply targeting Aβ after tau mediated spine loss has occurred is sufficient to ameliorate cognitive decline.

Acknowledgments

This work was supported by NIH grant AG027544 (FML), and NIA grant F31AG039968 (MAC). We thank the University of California, Irvine, Transgenic Mouse Facility and Tom Fielder for producing the transgenic founders of the $hAPP_{SL}$ and hTau lines. We thank Angelina Kang and Stephen Yeung for technical assistance.

ABBREVIATIONS

AD	Alzheimer’s disease
Aβ	amyloid-beta
APP	amyloid precursor protein

REFERENCES

Blurton-Jones M, Kitazawa M, Martinez-Coria H, Castello NA, Muller FJ, Loring JF, Yamasaki TR, Poon WW, Green KN, LaFerla FM. Neural stem cells improve cognition via BDNF in a transgenic

model of Alzheimer disease. Proc Natl Acad Sci U S A. 2009; 106:13594–13599. [PubMed: 19633196]

Carlson GA, Borchelt DR, Dake A, Turner S, Danielson V, Coffin JD, Eckman C, Meiners J, Nilsen SP, Younkin SG, Hsiao KK. Genetic modification of the phenotypes produced by amyloid precursor protein overexpression in transgenic mice. Hum Mol Genet. 1997; 6:1951–1959. [PubMed: 9302276]

Caroni P. Overexpression of growth-associated proteins in the neurons of adult transgenic mice. J Neurosci Methods. 1997; 71:3–9. [PubMed: 9125370]

Chabrier MA, Blurton-Jones M, Agazaryan AA, Nerhus JL, Martinez-Coria H, LaFerla FM. Soluble abeta promotes wild-type tau pathology in vivo. J Neurosci. 2012; 32:17345–17350. [PubMed: 23197725]

Chen Y, Rex CS, Rice CJ, Dube CM, Gall CM, Lynch G, Baram TZ. Correlated memory defects and hippocampal dendritic spine loss after acute stress involve corticotropin-releasing hormone signaling. Proc Natl Acad Sci U S A. 2010; 107:13123–13128. [PubMed: 20615973]

Chin J, Palop JJ, Yu GQ, Kojima N, Masliah E, Mucke L. Fyn kinase modulates synaptotoxicity, but not aberrant sprouting, in human amyloid precursor protein transgenic mice. J Neurosci. 2004; 24:4692–4697. [PubMed: 15140940]

DeKosky ST, Scheff SW. Synapse loss in frontal cortex biopsies in Alzheimer's disease: correlation with cognitive severity. Ann Neurol. 1990; 27:457–464. [PubMed: 2360787]

Deshpande A, Mina E, Glabe C, Busciglio J. Different conformations of amyloid beta induce neurotoxicity by distinct mechanisms in human cortical neurons. J Neurosci. 2006; 26:6011–6018. [PubMed: 16738244]

Dickstein DL, Brautigam H, Stockton SD Jr. Schmeidler J, Hof PR. Changes in dendritic complexity and spine morphology in transgenic mice expressing human wild-type tau. Brain Struct Funct. 2010; 214:161–179. [PubMed: 20213269]

Gotz J, Probst A, Spillantini MG, Schafer T, Jakes R, Burki K, Goedert M. Somatodendritic localization and hyperphosphorylation of tau protein in transgenic mice expressing the longest human brain tau isoform. EMBO J. 1995; 14:1304–1313. [PubMed: 7729409]

Holtmaat A, Wilbrecht L, Knott GW, Welker E, Svoboda K. Experience-dependent and cell-type-specific spine growth in the neocortex. Nature. 2006; 441:979–983. [PubMed: 16791195]

Hoover BR, Reed MN, Su J, Penrod RD, Kotilinek LA, Grant MK, Pitstick R, Carlson GA, Lanier LM, Yuan LL, Ashe KH, Liao D. Tau mislocalization to dendritic spines mediates synaptic dysfunction independently of neurodegeneration. Neuron. 2010; 68:1067–1081. [PubMed: 21172610]

Ittner LM, Ke YD, Delerue F, Bi M, Gladbach A, van Eersel J, Wolfing H, Chieng BC, Christie MJ, Napier IA, Eckert A, Staufenbiel M, Hardeman E, Gotz J. Dendritic function of tau mediates amyloid-beta toxicity in Alzheimer's disease mouse models. Cell. 2010; 142:387–397. [PubMed: 20655099]

Jack CR Jr. Knopman DS, Jagust WJ, Shaw LM, Aisen PS, Weiner MW, Petersen RC, Trojanowski JQ. Hypothetical model of dynamic biomarkers of the Alzheimer's pathological cascade. Lancet Neurol. 2010; 9:119–128. [PubMed: 20083042]

Kamenetz F, Tomita T, Hsieh H, Seabrook G, Borchelt D, Iwatsubo T, Sisodia S, Malinow R. APP processing and synaptic function. Neuron. 2003; 37:925–937. [PubMed: 12670422]

Kasai H, Matsuzaki M, Noguchi J, Yasumatsu N, Nakahara H. Structure-stability-function relationships of dendritic spines. Trends Neurosci. 2003; 26:360–368. [PubMed: 12850432]

Koffie RM, Hyman BT, Spires-Jones TL. Alzheimer's disease: synapses gone cold. Mol Neurodegener. 2011; 6:63. [PubMed: 21871088]

Lambert MP, Barlow AK, Chromy BA, Edwards C, Freed R, Liosatos M, Morgan TE, Rozovsky I, Trommer B, Viola KL, Wals P, Zhang C, Finch CE, Krafft GA, Klein WL. Diffusible, nonfibrillar ligands derived from Abeta1–42 are potent central nervous system neurotoxins. Proc Natl Acad Sci U S A. 1998; 95:6448–6453. [PubMed: 9600986]

Larson ME, Lesne SE. Soluble Abeta oligomer production and toxicity. J Neurochem. 2012; 120(Suppl 1):125–139. [PubMed: 22121920]

Lee G, Newman ST, Gard DL, Band H, Panchamoorthy G. Tau interacts with src-family non-receptor tyrosine kinases. J Cell Sci. 1998; 111(Pt 21):3167–3177. [PubMed: 9763511]

Lesne S, Koh MT, Kotilinek L, Kayed R, Glabe CG, Yang A, Gallagher M, Ashe KH. A specific amyloid-beta protein assembly in the brain impairs memory. Nature. 2006; 440:352–357. [PubMed: 16541076]

Mairet-Coello G, Courchet J, Pieraut S, Courchet V, Maximov A, Polleux F. The CAMKK2-AMPK kinase pathway mediates the synaptotoxic effects of Abeta oligomers through Tau phosphorylation. Neuron. 2013; 78:94–108. [PubMed: 23583109]

Mucke L, Selkoe DJ. Neurotoxicity of amyloid beta-protein: synaptic and network dysfunction. Cold Spring Harb Perspect Med. 2012; 2:a006338. [PubMed: 22762015]

Mucke L, Masliah E, Yu GQ, Mallory M, Rockenstein EM, Tatsuno G, Hu K, Kholodenko D, Johnson-Wood K, McConlogue L. High-level neuronal expression of abeta 1–42 in wild-type human amyloid protein precursor transgenic mice: synaptotoxicity without plaque formation. J Neurosci. 2000; 20:4050–4058. [PubMed: 10818140]

Oddo S, Caccamo A, Cheng D, Jouleh B, Torp R, LaFerla FM. Genetically augmenting tau levels does not modulate the onset or progression of Abeta pathology in transgenic mice. J Neurochem. 2007; 102:1053–1063. [PubMed: 17472708]

Perez-Cruz C, Nolte MW, van Gaalen MM, Rustay NR, Termont A, Tanghe A, Kirchhoff F, Ebert U. Reduced spine density in specific regions of CA1 pyramidal neurons in two transgenic mouse models of Alzheimer's disease. J Neurosci. 2011; 31:3926–3934. [PubMed: 21389247]

Pillai JA, Cummings JL. Clinical trials in predementia stages of Alzheimer disease. Med Clin North Am. 2013; 97:439–457. [PubMed: 23642580]

Querfurth HW, LaFerla FM. Alzheimer's disease. N Engl J Med. 2010; 362:329–344. [PubMed: 20107219]

Roberson ED, Scearce-Levie K, Palop JJ, Yan F, Cheng IH, Wu T, Gerstein H, Yu GQ, Mucke L. Reducing endogenous tau ameliorates amyloid beta-induced deficits in an Alzheimer's disease mouse model. Science. 2007; 316:750–754. [PubMed: 17478722]

Salter MW, Kalia LV. Src kinases: a hub for NMDA receptor regulation. Nat Rev Neurosci. 2004; 5:317–328. [PubMed: 15034556]

Spires TL, Meyer-Luehmann M, Stern EA, McLean PJ, Skoch J, Nguyen PT, Bacskai BJ, Hyman BT. Dendritic spine abnormalities in amyloid precursor protein transgenic mice demonstrated by gene transfer and intravital multiphoton microscopy. J Neurosci. 2005; 25:7278–7287. [PubMed: 16079410]

Terry RD, Masliah E, Salmon DP, Butters N, DeTeresa R, Hill R, Hansen LA, Katzman R. Physical basis of cognitive alterations in Alzheimer's disease: synapse loss is the major correlate of cognitive impairment. Ann Neurol. 1991; 30:572–580. [PubMed: 1789684]

Zempel H, Thies E, Mandelkow E, Mandelkow EM. Abeta oligomers cause localized Ca(2+) elevation, missorting of endogenous Tau into dendrites, Tau phosphorylation, and destruction of microtubules and spines. J Neurosci. 2010; 30:11938–11950. [PubMed: 20826658]

Highlights

- Novel transgenic models of Aβ and wild-type human tau pathology
- Knockdown of human APP ameliorates cognitive decline when human tau is not present
- Aβ-dependent acceleration of accumulation, aggregation and mislocalization of human wild-type tau
- Synergistic effect of both Aβ and wild-type tau on dendritic spine loss

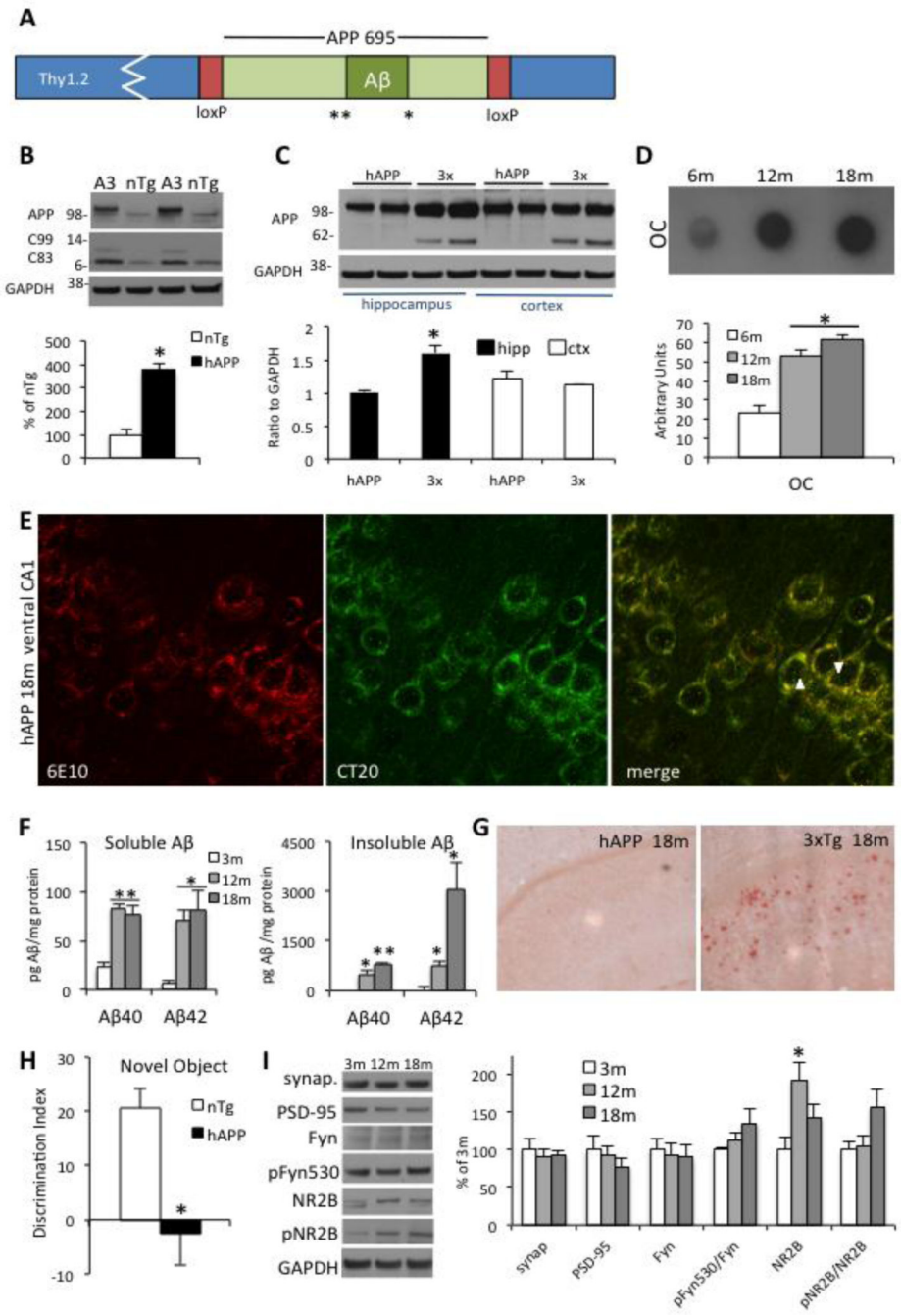

Figure 1. Novel hAPP$_{SL}$ mouse model exhibits increasing Aβ, oligomers and cognitive deficits without plaque deposition

A, Schematic diagram of hAPP$_{SL}$ transgene with Swedish**(KM670/671NL) and London*(V717I) mutations indicated. **B**, Western blot of founder A3 line compared to nontransgenic with an antibody that recognizes a conserved epitope between human and mouse APP (CT20) demonstrates approximately 4-fold overexpression of the hAPP$_{SL}$ protein. **C**, Comparison of human APP expression levels in the hemizygous hAPP$_{SL}$ mice versus homozygous 3xTg-AD mice shows greater expression in 3xTg-AD mice in the

hippocampus, but comparable levels in the cortex at 12 months of age. **D**, OC-positive pre-fibrillar oligomer levels increase with age (n=8 per group, *p<0.05 compared to 6m). **E**, Immunofluorescence staining of 18-month old $hAPP_{SL}$ mice for full-length APP (6E10, red) and C-terminal fragments (CT20, green) demonstrates accumulation pf APP and Aβ in CA1 pyramidal neurons. Intracellular Aβ, which is labeled by 6E10 but not CT20, is indicated by arrowheads. **F**, $hAPP_{SL}$ mice accumulate increasing levels of soluble and insoluble Aβ as measured by ELISA from cortical samples (n=8 per group, *p<0.05 compared to 3m, **p<0.01 compared to 3m). **G**, Despite the increases in Aβ and Aβ oligomers, no plaque deposition occurs as late as 18 months in hemizygous mice, as seen by staining with Congo Red compared to 3xTg-AD. **H**, At 12 months of age, $hAPP_{SL}$ mice show cognitive deficits in multiple cognitive tasks, including novel object recognition (n=8 per group). **I**, Despite the cognitive deficits, no changes are observed in the synaptic markers synaptophysin and PSD-95 with age in $hAPP_{SL}$ mice. However, there is an increase in NR2B subunits at 12 months, and a trend toward increased phosphorylated NR2B at 18 months (n=4 per group, *p<0.05 compared to 3m). Error bars +1 SEM for all graphs.

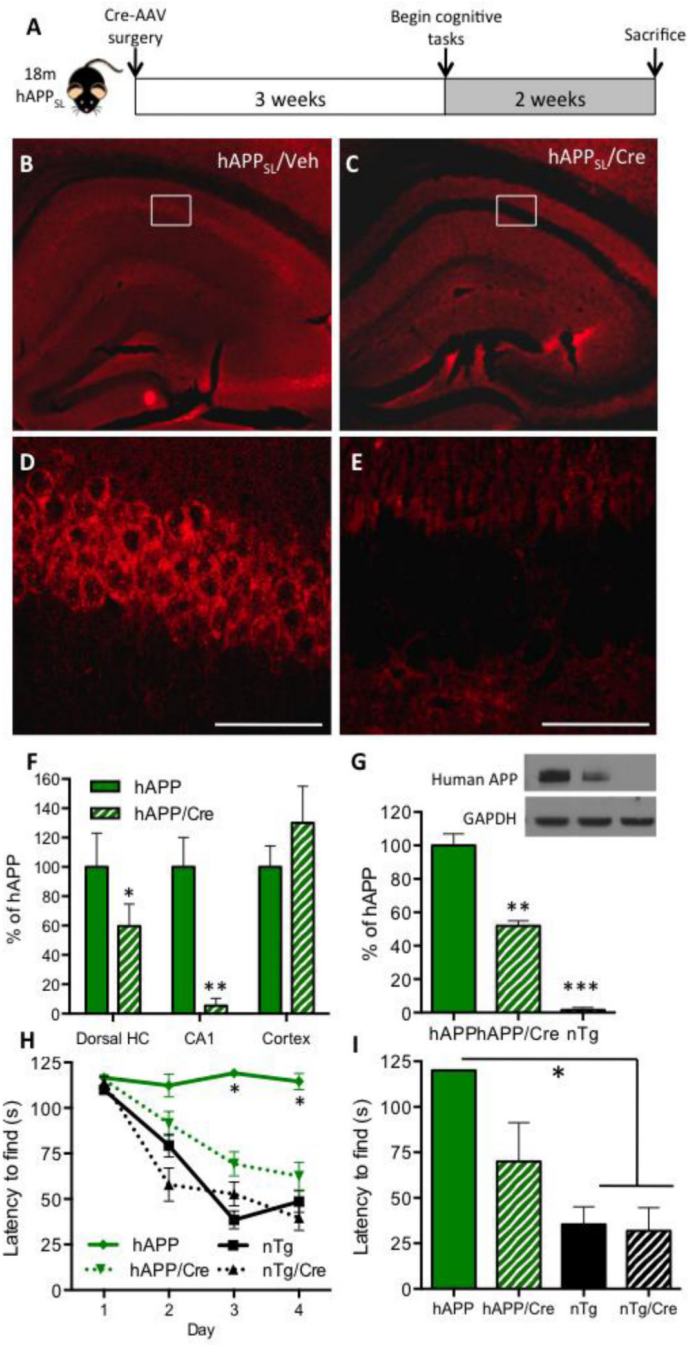

Figure 2. Knockdown of hAPP$_{SL}$ transgene expression by AAV-mediated delivery of Cre rescues cognition in aged mice

A, Study design. **B–E**, Five weeks post-injection, 18-month old hAPP$_{SL}$ mice injected with vehicle show robust APP expression in CA1, while mice injected with AAV expressing Cre recombinase have a remarkable reduction in human APP expression in the dorsal hippocampus (B and D- vehicle, C and E- Cre). **F**, Quantification of steady states human APP levels shows almost complete reduction of APP in CA1 pyramidal cells, but no change in cortical areas. **G**, Biochemical analysis of APP levels in microdissected hippocampal

lysates shows a 50% reduction of human APP. **H**, $hAPP_{SL}$ mice injected with either vehicle or Cre virus were tested for cognition by Barnes Maze. By days 3 and 4, $hAPP_{SL}$/Cre mice learned to find the escape hole significantly faster than $hAPP_{SL}$/Veh mice, performing almost at wild-type levels. **I**, Memory for the escape hole location was assessed 24-hours after the final learning trial. $hAPP_{SL}$/Cre mice showed strong memory for the platform location, finding the escape hole in approximately 1 minute, while $hAPP_{SL}$/Veh mice never attempted to enter the correct hole. N=6–10 per group, *$p<0.05$ and **$p<0.01$ compared to nTg Veh. Error bars +1 SEM for all graphs.

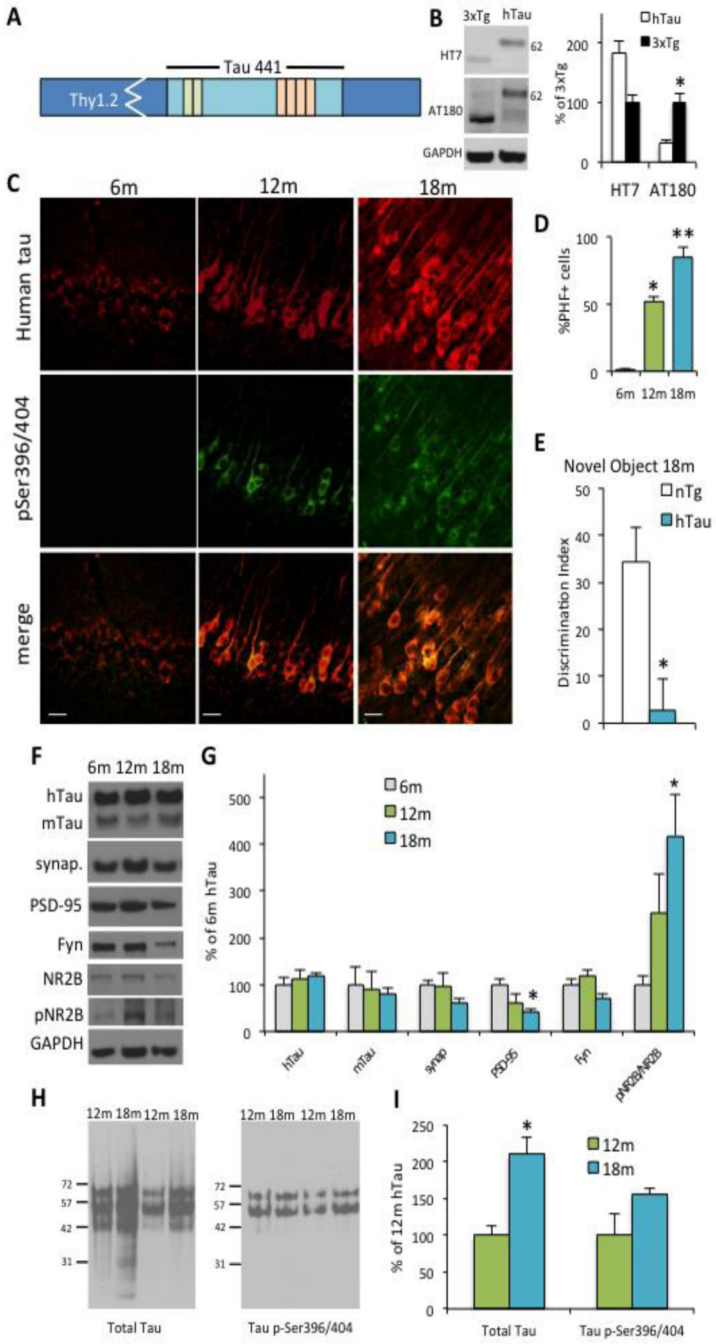

Figure 3. Generation of hTau mouse to study Aβ-dependent and independent effects on wild-type tau pathology

A, Schematic design of full-length human tau, 4R/2N, transgene. **B**, Total tau levels (HT7) are trending toward an increase in hemizygous hTau mice compared to homozygous 3xTg-AD mice at 4 months. Levels of tau phosphorylated at Thr231/Ser235 (AT180) are increased in 3xTg-AD, which is expected due to the presence of the human APP transgene. 3xTg-AD mice harbor 4R/0N tau with the P301L mutation. **CâD**, Somatodendritc, phosphorylated tau is evident in multiple brain regions such as the amygdala, hippocampus

and cortex. Here, we show that tau mislocalization and hyperphosphorylation increase with age in hTau mice, with approximately 85% of tau positive cells containing hyperphosphorylated PHF-1 tau by 18 months in CA1 neurons. **E**, The first observed memory deficits occur at 18-months in hTau mice. These mice exhibit memory deficits in novel object recognition compared to age-matched nontransgenic mice, corresponding with the time point of enhanced dendritic tau localization and decreased PSD-95. (n=8 per group) **F–G**, Steady state levels of total tau remain constant with age, but there is a significant decrease in the level of postsynaptic marker PSD-95. Interestingly, there is corresponding increase in the both the levels and phosphorylated state of NMDAR NR2B subunits. (n=4–5 per group, *$p<0.05$ compared to 6m hTau) **H–I**, Interestingly, insoluble tau levels are significantly increased in 18-month hTau mice compared to 12-month hTau mice in cortical samples. No differences were seen in levels of tau phosphorylation in the insoluble fraction. Scale bars represent 20 μm in all images.

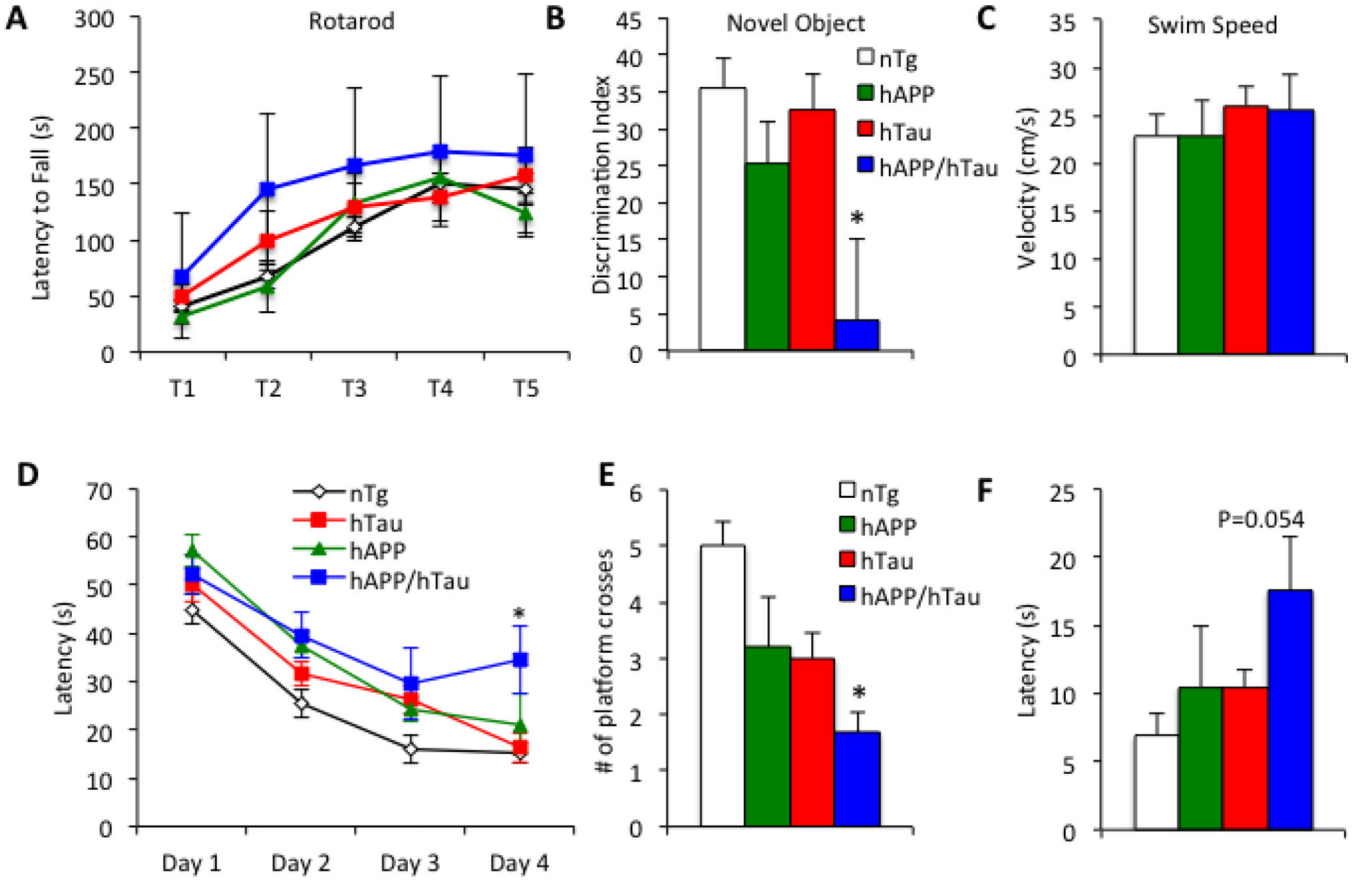

Figure 4. Acceleration of cognitive deficits in double transgenic hAPP$_{SL}$/hTau mice

A, Importantly, no differences in motor skills were found between all groups of nontransgenic, single transgenic and double transgenic mice, as tested by five 5-minute trials (T1-T5) on the Rotarod. **B**, Mice were also analyzed for hippocampus-independent cognition using novel object recognition. Nontransgenic, hAPP$_{SL}$, and hTau groups all displayed preference for the novel object, indicating they remembered the old object from training, while hAPP$_{SL}$/hTau showed no preference and therefore no memory for the old object. **C–E**, All groups were tested for hippocampus dependent memory using Morris water maze. No differences were found in swim speed (C). hAPP$_{SL}$/hTau mice showed significant deficits in learning the platform location compared to nTg mice on Day 4 (D), and also showed memory deficits for the platform location on the 24-hour probe trial (E). A trend toward increased latency to the platform location was also found in hAPP$_{SL}$/hTau mice compared to nTg. (n=10 nTg, n=6 hAPP, n=8 hTau, n=4 hAPP$_{SL}$/hTau)

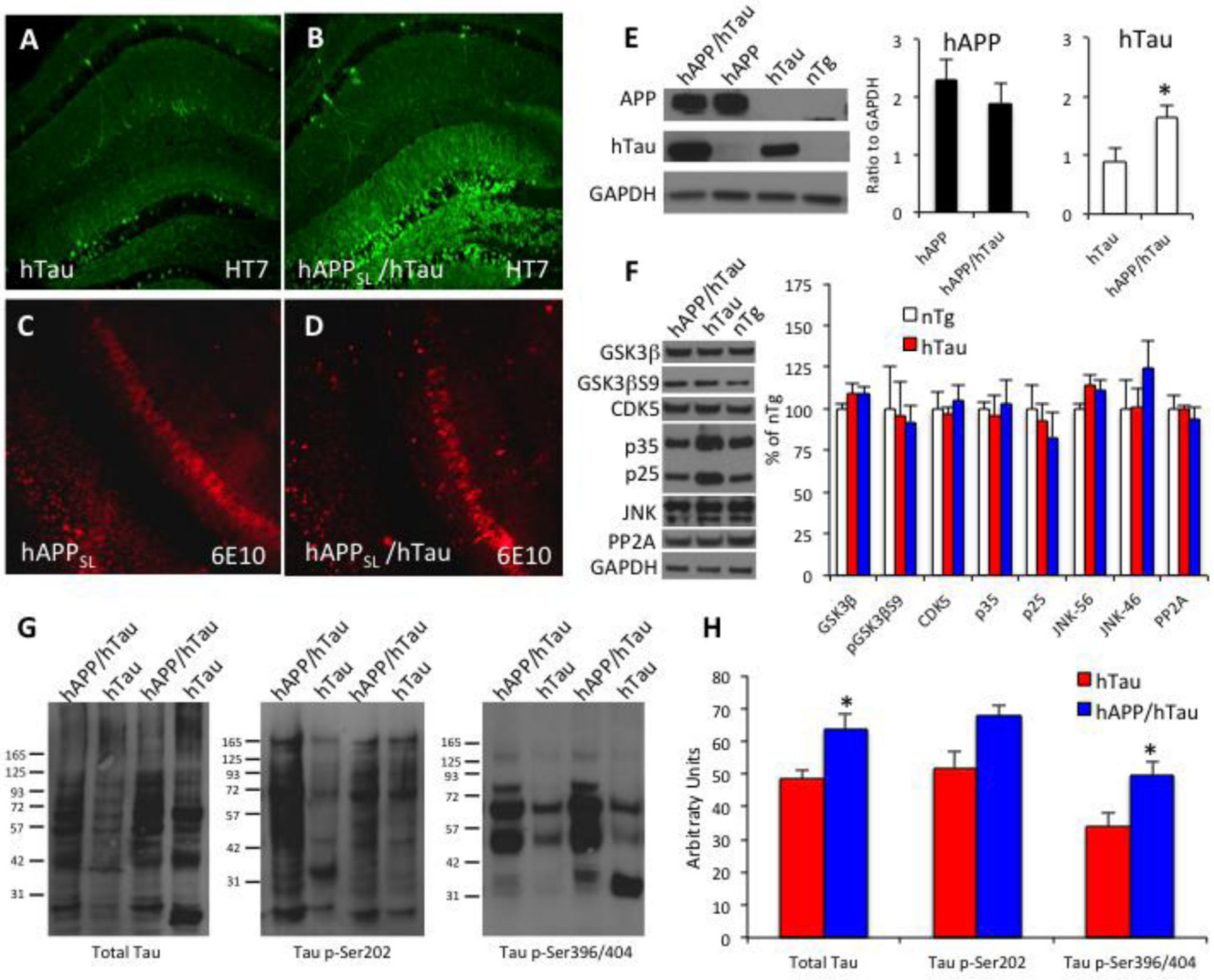

Figure 5. Human APP expression augments wild-type tau pathology

A–D, Staining for total human tau and human APP revealed an increased in hTau expression in the hippocampus of hAPP$_{SL}$/hTau mice, specifically in the granule cells of the dentate gyrus. No differences were observed in levels of APP. **E**, Quantification of protein levels by western blot analysis of hippocampal lysates confirmed the increase in human tau, but not human APP in double transgenic mice. **F**, Interestingly, no changes were seen in levels of phosphorylated tau (not shown), or in the major tau kinases GSK3β, CDK5 or JNK in soluble hippocampal lysates (n=4 per group) **G–H**, However, levels of total tau and phosphorylated tau, in monomeric, aggregated, and cleaved forms, were increased in the insoluble fraction of hippocampal lysates in hAPP$_{SL}$/hTau mice compared to single transgenic hTau mice.

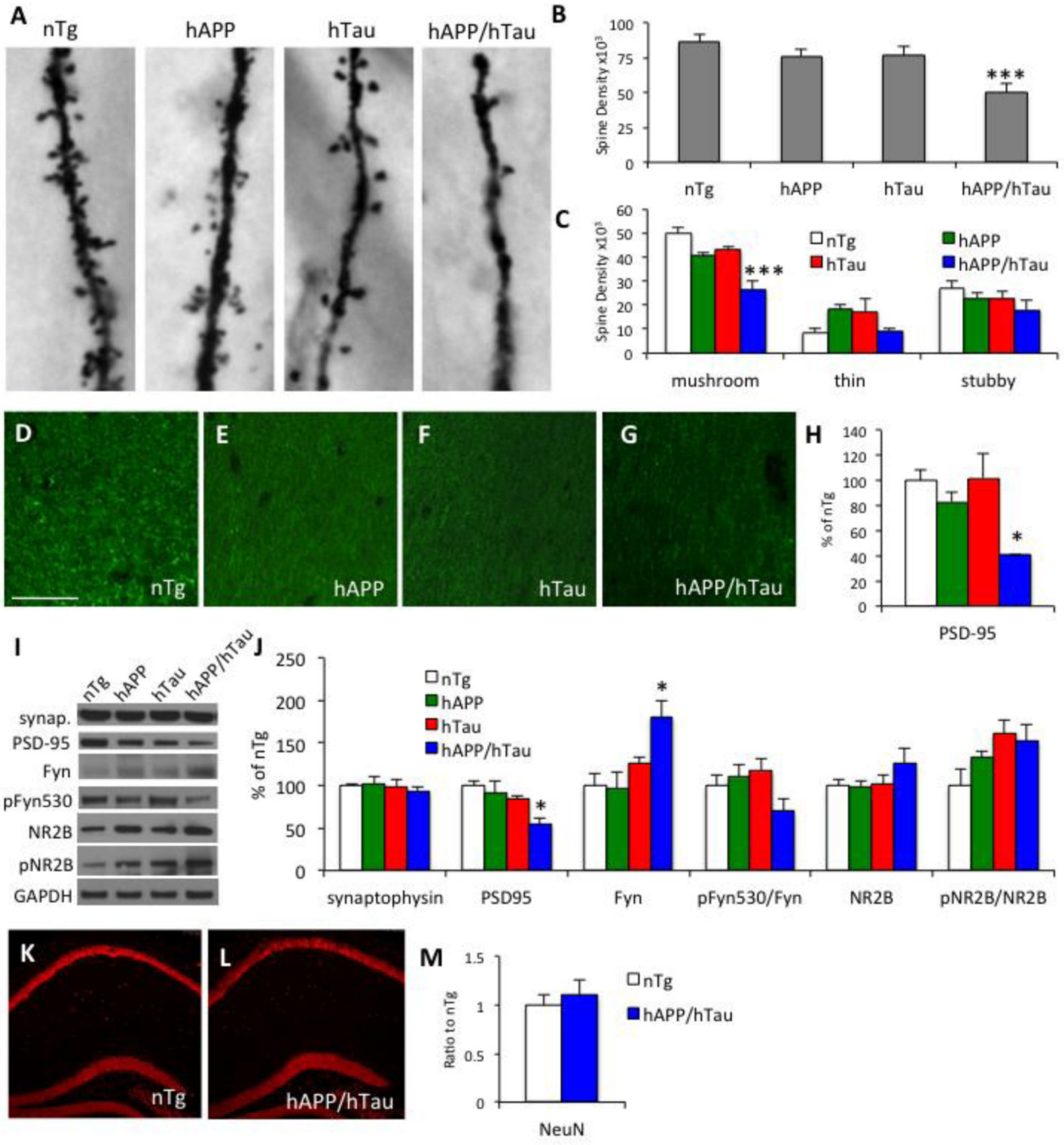

Figure 6. Decreased spine density but no overt neuronal loss in hAPP$_{SL}$/hTau mice

A–C, Golgi staining revealed a dramatic loss in the number of spines in hAPP$_{SL}$/hTau mice in the stratum radiatum layer of the hippocampus compared to all other groups at 8 months of age (B). A representative dendrite is shown from each group (A). Classification of these spines suggests that the majority of spine loss in hAPP$_{SL}$/hTau mice is due to a loss of mature mushroom spines. **D–H**, To further investigate synaptic changes, sections from each group were stained for PSD-95 (shown) and synaptophysin (not shown), and the number of puncta in the stratum radiatum was counted in each section. Interestingly, hAPP$_{SL}$/hTau

mice showed a 60% decrease in PSD-95 puncta (G–H), while no differences in synaptophysin were observed. **I–J**, Biochemical analysis of hippocampal lysates confirmed the decrease in PSD-95, and also demonstrated a significant increase in the protein kinase Fyn, which has been implicated in AD synaptotoxicity. Despite the marked loss of spines, NR2B and pNR2B-1472 still trended to increase in $hAPP_{SL}$/hTau mice. **K–M**, To check if the observed spine loss could be due to a loss of CA1 pyramidal cells, $hAPP_{SL}$/hTau and nontransgenic mice were stained with NeuN. No difference in the intensity of the stain was observed. (*$p<0.05$, ***$p<0.001$ compared to nTg, n=4 per group)